Optimal Control of Multi-Dimensional, Hybrid Ice-Skater Model

Tejas R. Mehta, Deryck Yeung, Erik I. Verriest, Magnus Egerstedt

***Abstract*— In this paper, we study hybrid models that not only undergo mode transitions, but also experience changes in dimensions of the state and input spaces. An algorithmic framework for the optimal control of such Multi-Mode, Multi-Dimension (or M^3D) systems is presented. We moreover derive a detailed M^3D model for an ice-skater, and demonstrate the use of the developed framework on the ice-skater model.**

I. INTRODUCTION

Hybrid systems, i.e. systems whose dynamics contain both a continuous and a discrete component, have proved to be useful tools when modelling complex physical systems, where the dynamics changes among different dynamical regimes in response to external as well as internal events. Examples range from bipedal, walking robots [1], where each leg undergoes a swing-phase and a stance-phase, and high-velocity mobile robots [2], where the wheels transition between rolling and slipping modes, to models in systems biology [3], [4], in which regulatory networks inhibit or excite different aspects of the cell dynamics. This paper follows this tradition by focusing on constrained (physical) systems (see for example [5]). However, rather than focusing on modelling and analysis, we make the control of these systems the explicit aim.

Unfortunately, producing computationally feasible algorithms for hybrid control design has proved to be a daunting task from a complexity point of view. As an example, one can consider the problem of optimal control of hybrid systems, where [6], [7] early on formulated variants of the hybrid maximum principle. However, the leap from optimality conditions to computational algorithms has proved computationally infeasible except for restricted problem classes, such as piecewise affine systems [8], systems in which the mode schedule is predetermined [9], [10], to classes of suboptimal solution methods [11], [12].

In this paper, we make no claims about solving the general, hybrid optimal control problem, but rather focus our attention on systems for which the mode sequence is fixed and given. The control parameters then becomes the control signals within each individual mode and parameterized characterizations of the switching conditions and transition relations. This work can be viewed as an extension of [13]. In [13] a new class of systems, the so-called Multi-Mode, Multi-Dimension (or M^3D), was introduced where the dimension of the system is allowed to change from mode to mode. Furthermore, various state transition maps and an optimal control problem were considered. In this paper, however, we will, as an extension, also allow the dimension of the control space to change as the system undergoes mode switchings. Due to the possible changes of dimensions in the control and state space, it is necessary to introduce a new computational algorithm to implement the optimality conditions. Although it is possible to embed this algorithm into a more classical and larger algorithm, our approach has the advantage that it is significantly less demanding in terms of computational time and complexity because only relevant variables are computed. Moreover, we will consider a fairly elaborate model of a ice-skater to illustrate the modeling and control of M^3D systems. This skating model will operate in four different modes as the skater moves forward, where each mode characterizes the particular motion of both skates. A corresponding optimal control problem will be considered as well.

The outline of this paper is as follows: In Section II, the ice-skater model will be introduced as a vehicle for illustrating the various modelling issues. Following this, in Section III, M^3D systems will be formally introduced and optimality conditions will be derived within the framework of the Calculus of Variations. This section moreover contains a description of the development of a computational algorithm, which is then applied to the ice-skater model in Section IV. The conclusions are given in Section V.

II. A MOTIVATING EXAMPLE

In this section, we introduce a M^3D model for an ice-skater. Figure (1) shows the trajectories of both the left and right skate (dotted lines) with respect to the forward motion (from left to right).The human body is modelled by three masses; m for each leg and M for the torso and head. The skating motion is modelled as a M^3D system having four modes. These modes are the 'Stride-Right' (SR) mode, the 'Glide-Left' (GL) mode, the 'Stride-Left' (SL) and the 'Glide-Right' (GR) mode. The detailed dynamics of each mode are presented next.

- *SL mode*:
  Throughout the skating motion, the angles of the left and the right skate with respect to the x-axis are denoted by α_l and α_r, respectively.
  During this mode, the skater applies a force u on the right skate along the line of the body as shown in figure (2). The mass of the torso (M) and of the right leg (m) are assumed to be resting on the left skate during this acceleration. Therefore, the total mass going along the left skate is $m+M$. Accordingly, the mass on the right skate is m. As the right skate pushes outward, the same

The authors are with the School of Electrical and Computer Engineering, Georgia Institute of Technology, Atlanta, GA 30332, USA {tmehta, deryck, erik.verriest, magnus}@ece.gatech.edu

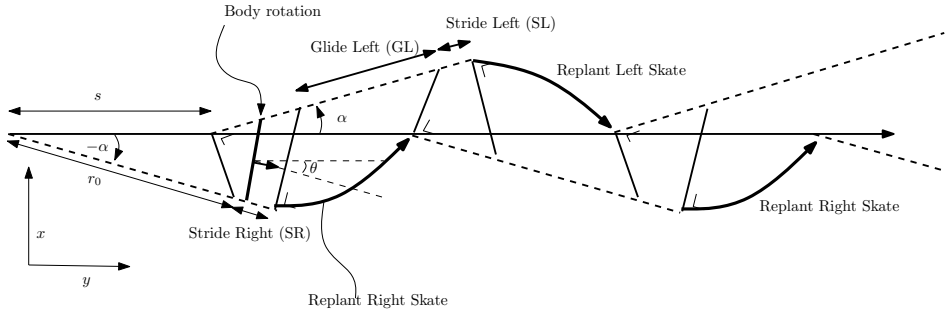

Fig. 1. Skating trajectories using the proposed M^3D model.

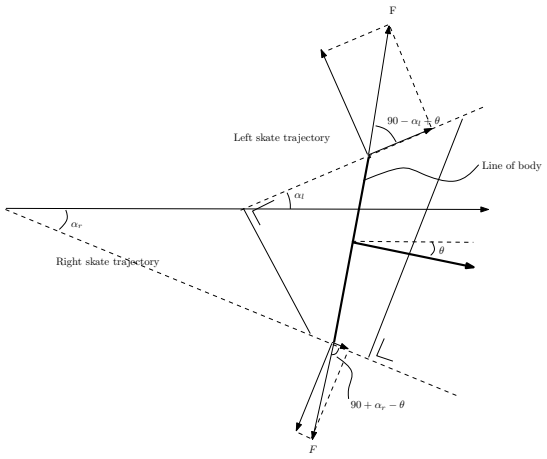

Fig. 2. Depicted is the force applied during the SL mode

force is being applied to the right and left skate by the ice, but in the opposite direction. The components perpendicular to each skate edge are cancelled by the forces normal in the plane. The remaining components along the skate edge are responsible for the forward motion. The friction between the ice and both skates is proportional to the normal force. The proportionality constant, in turn, is a function of the velocity [14]. This friction, however, is significantly smaller than air friction that accounts for 75% of the resistance [14]. The air friction force satisfies $\mu_k v^2$, where μ_k is a constant depending on the drag coefficient, frontal area, and the posture of the skater [16]. A physical constraint is the distance R, $R = \sqrt{(x_l - x_r)^2 + (y_l - y_r)^2}$ between the two skates. Furthermore, the heading angle θ is constrained to be $\alpha_l \leq \theta \leq \alpha_r$. Using Newton's second law, the state equations are readily obtained:

$$\begin{aligned}
\dot{x}_l &= v_l \cos(\alpha_l) \\
\dot{y}_l &= v_l \sin(\alpha_l) \\
\dot{v}_l &= \frac{u}{m+M} \sin(\alpha_l - \theta) - \frac{\mu_k}{m+M} v_c^2 \\
\dot{x}_r &= v_r \cos(\alpha_r) \\
\dot{y}_r &= v_r \sin(\alpha_r) \\
\dot{v}_r &= \frac{u}{m} \sin(\alpha_r - \theta) - \frac{\mu_k}{m} v_c^2
\end{aligned}$$

where μ_k is the air friction coefficient and $v_c = \frac{(m+M)v_l + m v_r}{M+2m}$ is the velocity of the center mass. Also, the heading angle $\theta = \tan^{-1}(\frac{x_l - x_r}{y_l - y_r})$.

- *GL mode*:
  This mode is the continuation of the previous mode, where the skater rests on his left skate while the right skate is lifted in the air for repositioning. The state equations, obtained by setting the applied forces to zero in the previous mode, are

$$\begin{aligned}
\dot{x}_l &= v_l \cos(\alpha_l) \\
\dot{y}_l &= v_l \sin(\alpha_l) \\
\dot{v}_l &= -\frac{\mu_k}{M+2m} v_l^2
\end{aligned}$$

- *SR mode*:
  After the right skate has been replanted, the right skate begins its striding phase, while the left skate applies the force. This is similar to the SL mode with the role reversal between the left and right skates. The state equations are

$$\begin{aligned}
\dot{x}_l &= v_l \cos(\alpha_l) \\
\dot{y}_l &= v_l \sin(\alpha_l) \\
\dot{v}_l &= \frac{u}{m} \sin(\theta - \alpha_l) - \frac{\mu_k}{m} v_c^2 \\
\dot{x}_r &= v_r \cos(\alpha_r) \\
\dot{y}_r &= v_r \sin(\alpha_r) \\
\dot{v}_r &= \frac{u}{m+M} \sin(\theta - \alpha_r) - \frac{\mu_k}{m+M} v_c^2
\end{aligned}$$

  where $v_c = \frac{m v_l + (m+M) v_r}{M+2m}$.

- *GR mode*:
  The end of the previous mode leads to the Glide-Right mode, where the skater glides on his right skate. This is the right skate analogue of the 'GL mode,' and the corresponding state equations are

$$\begin{aligned}
\dot{x}_r &= v_r \cos(\alpha_r) \\
\dot{y}_r &= v_r \sin(\alpha_r) \\
\dot{v}_r &= -\frac{\mu_k}{M+2m} v_r^2
\end{aligned}$$

The boundary conditions at mode switching instants can be determined by physical arguments. Assuming the conservation of momentum, the velocity of the left skate at the onset of the GL from SL mode is $v_l^+ = \frac{m v_r^- + (M+m) v_l^-}{M+2m}$. Since the position of left skate is determined from the end of SL, the position of the left skate at the onset of GL satisfies $x_l^+ = x_l^-$ and $y_l^+ = y_l^-$. We further denote this set

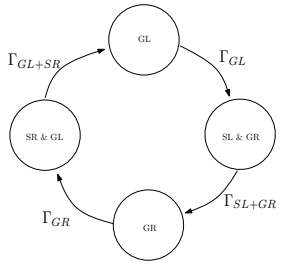

Fig. 3. State Transition

of conditions F_{SL}. During the GL mode, the right skate is being repositioned a distance of r_x units forward to prepare for the SR mode. Therefore, at the onset of the SR mode, $x_r^+ = x_l^- + r_x$ and $y_r^+ = y_l^- - r_y$. Furthermore, the position and velocity of the left skate continues from the end of GL. Hence, $x_l^+ = x_l^-$, $y_l^+ = y_l^-$, $v_l^+ = v_l^-$, and $v_r^+ = v_l^-$.We denote this transition map as F_{GL}. By similar arguments, the transition map F_{SR} from the SR mode to the GR mode is $x_r^+ = x_r^-$, $y_r^+ = y_r^-$, $v_r^+ = \frac{(m+M)v_r + mv_l}{M+2m}$, and the transition map F_{GR} from GR to SL is $x_l^+ = x_r^- + r_x$, $y_l^+ = y_r^- + r_y$, $v_l^+ = v_r^-$, $x_r^+ = x_r^-$, $y_r^+ = y_r^-$, and $v_r^+ = v_r^-$.

III. OPTIMALITY CONDITIONS

Having motivated the need for optimal control of multi-dimensional hybrid systems in the previous section, in this section we begin by formalizing the optimal control problem. Then we use variational arguments to derive the necessary conditions for optimality. Once these conditions are obtained, we will present a numerical algorithm that utilizes these optimality conditions to converge to a local solution for the optimal control parameters.

A. Problem Formulation

The dynamical system discussed in this paper corresponds to a specific class of hybrid systems, where the dimension of the state and control space changes between different modes of operation. We assume that switches between the different dynamics is time-driven, where the switching-time vector $\vec{\tau} = [\tau_1, \ldots, \tau_{N-1}]^T$ is also a control parameter. However, the ordering of the modes is assumed fixed. Also, the initial time $\tau_0 = 0$ and final time $\tau_N = T$ will be assumed fixed. It will be beneficial to introduce an identifier $p(i)$, taking values in a finite set, denoting the mode of operation during the time interval $[\tau_{i-1}, \tau_i)$. As mentioned earlier, the dimensions of the state and control spaces vary from mode to mode. Hence, we let $x^{p(i)} \in \mathbb{R}^{n^{p(i)}}$, while $u^{p(i)} \in \mathbb{R}^{m^{p(i)}}$. Now, the state evolution during time interval $[\tau_{i-1}, \tau_i)$ is given by

$$\dot{x}^{p(i)} = f^{p(i)}(x^{p(i)}(t), u^{p(i)}(t)), \tag{1}$$

where $f^{p(i)} \in \mathcal{C}^2 : \mathbb{R}^{n^{p(i)}} \times \mathbb{R}^{m^{p(i)}} \to \mathbb{R}^{n^{p(i)}}$ is a twice-differentiable continuous-state transition function in mode $p(i)$. Thus the control, thus far, consists of a continuous time input $u^{p(i)}(\cdot)$ for each mode $p(1), \ldots, p(N)$ and the switching time vector $\vec{\tau}$.

Note that since the state trajectory switches between different dimensions, the state trajectories are discontinuous at the switching instants. The transition functions at the switching time instants are given as

$$x^{p(i+1)}(\tau_i+) = F^{p(i)}(x^{p(i)}(\tau_i-), w^{p(i)}), \tag{2}$$

for $i = 1, \ldots, N$. Here, $F^{p(i)} \in \mathcal{C}^2 : \mathbb{R}^{n^{p(i)}} \times \mathbb{R}^{k^{p(i)}} \to \mathbb{R}^{n^{p(i+1)}}$ is a twice-differentiable discrete-state transition function, and $w^{p(i)} \in \mathbb{R}^{k^{p(i)}}$ is a control parameter. For ease of notation, let's parameterize the state and control vectors by their sequential index rather than the identifier $p(i)$. Thus if we start with the initial state $x_1(0)$, the state trajectory will be given as follows:

$$\dot{x}_i(t) = f_i(x_i(t), u_i(t)), \text{ when } t \in [\tau_{i-1}, \tau_i) \tag{3}$$

$$x_{i+1}(\tau_i+) = F_i(x_i(\tau_i), w_i), \tag{4}$$

for $i = 1, \ldots, N$. Note here once again, that $x_i \in \mathbb{R}^{n_i}$, $u_i \in \mathbb{R}^{m_i}$ when $t \in [\tau_{i-1}, \tau_i)$, and $w_i = \mathbb{R}^{k_i}$.

Now that we have a characterization of the state trajectory, we can formulate an optimal control problem. More specifically, the problem is to determine the optimal continuous control signal $u_i(t)$ for $i = 1, \ldots, N$, discrete control signal w_i for $i = 1, \ldots, N-1$, and switching time vector $\vec{\tau} = [\tau_1, \ldots, \tau_{N-1}]^T$ in order to minimize a performance index

$$J = \sum_{i=1}^{N} \int_{\tau_{i-1}}^{\tau_N} L_i(x_i, u_i)dt + \sum_{i=1}^{N-1} \phi_i(x_i(\tau_i-), w_i) + \Phi(x_N(\tau_N)) \tag{5}$$

Here $L_i \in \mathcal{C}^2 : \mathbb{R}^{n_i} \times \mathbb{R}^{m_i} \to \mathbb{R}$ is the instantaneous cost in mode i, while $\phi_i \in \mathcal{C}^2 : \mathbb{R}^{n_i} \times \mathbb{R}^{k_i} \to \mathbb{R}$ is a state transition cost between modes and $\Phi \in \mathcal{C}^2 : \mathbb{R}^{n_N} \to \mathbb{R}$ is the terminal cost. In the next subsection, we will derive the optimal control via calculus of variations.

B. Optimality Conditions

In this section, we derive the optimality conditions for the problem defined above using a variational approach. This approach avoids the explicit computation of the perturbations with a clever choice of the Lagrange multipliers. Adjoining the dynamical constraints (3) to the cost (5) via different Lagrange multipliers (or co-states), $\lambda_i(t) \in \mathbb{R}^{1 \times n_i}$, defined over time interval (τ_{i-1}, τ_i), will not alter the value of J. Moreover, by adjoining the state transition constraints at the switching times (4) via Lagrange multipliers $\mu_i \in \mathbb{R}^{1 \times n_{i+1}}$, and assuming that the optimal control variables are chosen, we obtain the optimal cost $\bar{J}_0$.

Defining the Hamiltonians, $H_i(x_i, \lambda_i, u_i) = L_i(x_i, u_i) + \lambda_i f_i(x_i, u_i)$, the augmented (but unaltered from an evaluation point of view) cost is given by

$$\bar{J}_0 = \sum_{i=1}^{N} \int_{\tau_{i-1}}^{\tau_i} \Big[H_i(x_i, \lambda_i, u_i) - \lambda_i \dot{x}_i \Big] dt + \tag{6}$$

$$+ \sum_{i=1}^{N-1} \mu_i \Big[F_i(x_i(\tau_i-), w_i) - x_{i+1}(\tau_i+) \Big] + \sum_{i=1}^{N} \phi_i(x_i(\tau_i-), w_i).$$

In the equation above, we let $\phi_N(x_N(\tau_N-), w_N) = \Phi_N(x_n(\tau_N))$.

Now we perturb (6) in such a way that $u_i \to u_i + \epsilon\nu_i$ for $i = 1, \ldots, N$, $\tau_i \to \tau_i + \epsilon\theta_i$ and $w_i \to w_i + \epsilon\omega_i$ for $i = 1, \ldots, N-1$. With $\epsilon << 1$, this perturbation induces a

sequence of perturbations $\{\eta_i\}$ in the state trajectories x_i, e.g. $x_i \to x_i + \epsilon\eta_i$. Note that $\theta_0 = \theta_N = 0$ since the initial and final times are assumed fixed. The first order approximation of the perturbed cost, $\bar{J}_\epsilon$, is given by

$$\begin{aligned}\bar{J}_\epsilon=&\sum_{i=1}^{M}\int_{\tau_{i-1}}^{\tau_i}\Big[H_i(x_i,\lambda_i,u_i)-\lambda_i\dot{x}\Big]dt+\sum_{i=1}^{N}\int_{\tau_i}^{\tau_i+\epsilon\theta_i}L_i(x_i,u_i)dt-\\
&-\sum_{i=1}^{N}\int_{\tau_{i-1}}^{\tau_{i-1}+\epsilon\theta_{i-1}}L_i(x_i,u_i)dt+\epsilon\sum_{i=1}^{N}\int_{\tau_{i-1}}^{\tau_i}\Big[\frac{\partial H_i}{\partial x_i}\eta_i+\frac{\partial H_i}{\partial u_i}\nu_i-\lambda_i\dot{\eta}_i\Big]dt\\
&+\sum_{i=1}^{N-1}\mu_i\Big[F_i\big((x_i(\tau_i+\epsilon\theta_i)-),w_i+\epsilon\omega_i\big)-x_{i+1}(\tau_i+\epsilon\theta_i)+)\Big]\\
&+\epsilon\sum_{i=1}^{N-1}\mu_i\Big[\frac{\partial F_i}{\partial x_i}\eta_i(\tau_i-)-\eta_{i+1}(\tau_i+)\Big]+\qquad(7)\\
&+\sum_{i=1}^{N}\phi_i\big((x_i((\tau_i+\epsilon\theta_i)-),w_i+\epsilon\omega_i\big)+\epsilon\sum_{i=1}^{N}\frac{\partial\phi_i}{\partial x_i}\eta(\tau_i-).\end{aligned}$$

Note that we explicitly used the fact that $f_i(x_i(t),u_i(t)) - \dot{x}_i(t)$ is zero in the open intervals $(\tau_{i-1},\tau_{i-1}+\epsilon\theta_{i-1})$ and $(\tau_i,\tau_i+\epsilon\theta_i)$.

Now the first variation in the performance index (5) can be expressed as the limit for $\epsilon \to 0$ of

$$\delta J = \lim_{\epsilon\to 0}\frac{\bar{J}_\epsilon - \bar{J}_0}{\epsilon}. \qquad (8)$$

Thus using (6) and (7), it follows that

$$\begin{aligned}\delta J=&\sum_{i=1}^{N}\int_{\tau_{i-1}}^{\tau_i}\Big[\frac{\partial H_i}{\partial x_i}\eta_i+\frac{\partial H_i}{\partial u_i}\nu_i-\lambda_i\dot{\eta}_i\Big]dt+\\
&+\sum_{i=1}^{N}L_i(x_i,u_i)|_{\tau_i}\theta_i-L_i(x_i,u_i)|_{\tau_{i-1}}\theta_{i-1}+\\
&+\sum_{i=1}^{N-1}\mu_i\Big[\frac{\partial F}{\partial x_i}\dot{x}_i(\tau_i-)\theta_i+\frac{\partial F}{\partial w_i}\omega_i-\dot{x}_{i+1}(\tau_i+)\theta_i\Big]+\\
&+\sum_{i=1}^{N-1}\mu_i\Big[\frac{\partial F_i}{\partial x_i}\eta_i(\tau_i-)-\eta_{i+1}(\tau_i+)\Big]+\\
&+\sum_{i=1}^{N}\Big[\frac{\partial\phi_i}{\partial x_i}\dot{x}_i(\tau_i-)\theta_i+\frac{\partial\phi_i}{\partial w_i}\omega_i+\frac{\partial\phi_i}{\partial x_i}\eta(\tau_i-)\Big].\qquad(9)\end{aligned}$$

Reordering the sum, reorganizing terms, and remembering that $\theta_0 = \theta_N = 0$, we get

$$\begin{aligned}\delta J=&\sum_{i=1}^{N}\int_{\tau_{i-1}}^{\tau_i}\Big[\frac{\partial H_i}{\partial x_i}\eta_i+\frac{\partial H_i}{\partial u_i}\nu_i-\lambda_i\dot{\eta}_i\Big]dt+\sum_{i=1}^{N-1}\Big[L_i(x_i,u_i)\\
&-L_{i+1}(x_{i+1},u_{i+1})\Big]_{\tau_i}\theta_i+\sum_{i=1}^{N-1}\Big[\mu_i\frac{\partial F}{\partial x_i}f_i(\tau_i-)-\mu_i f_{i+1}(\tau_i+)\\
&+\frac{\partial\phi_i}{\partial x_i}f_i(\tau_i-)\Big]\theta_i+\sum_{i=1}^{N-1}\mu_i\Big[\frac{\partial F_i}{\partial x_i}\eta_i(\tau_i-)-\eta_{i+1}(\tau_i+)\Big]+\\
&+\sum_{i=1}^{N-1}\frac{\partial F}{\partial w_i}\omega_i+\sum_{i=1}^{N}\Big[\frac{\partial\phi_i}{\partial w_i}\omega_i+\frac{\partial\phi_i}{\partial x_i}\eta(\tau_i-)\Big].\qquad(10)\end{aligned}$$

Using integration by parts, the integral terms in (10) further reduces to

$$\begin{aligned}\delta\mathcal{K}=&\sum_{i=1}^{N}\int_{\tau_{i-1}}^{\tau_i}\Big[\frac{\partial H_i}{\partial x_i}\eta_i+\frac{\partial H_i}{\partial u_i}\nu_i-\dot{\lambda}_i\eta_i\Big]dt-\\
&-\sum_{i=1}^{N}\Big[\lambda_i(\tau_i-)\eta_i(\tau_i-)-\lambda_i(\tau_{i-1}+)\eta_i(\tau_{i-1}+)\Big]\qquad(11)\end{aligned}$$

Substituting $\delta\mathcal{K}$ into δJ, and choosing λ_i in the intervals (τ_{i-1},τ_i) to solve

$$\dot{\lambda}_i = -\frac{\partial H_i}{\partial x_i}(x_i,\lambda_i,u_i), \qquad (12)$$

yields

$$\begin{aligned}\delta J=&\sum_{i=1}^{N}\int_{\tau_{i-1}}^{\tau_i}A_i\nu_i dt+\sum_{i=1}^{N-1}B_i\omega_i+\sum_{i=1}^{N-1}C_i\theta_i+\\
&+\sum_{i=1}^{N-1}\Big[\lambda_{i+1}(\tau_i+)-\mu_i\Big]\eta_{i+1}(\tau_{i+1}+)+\\
&+\sum_{i=1}^{N-1}\Big[\mu_i\frac{\partial F_i}{\partial x_i}+\frac{\partial\phi_i}{\partial x_i}-\lambda_i(\tau_i-)\Big]\eta_i(\tau_i-)+\\
&+\Big[\frac{\partial\Phi}{\partial x_N}-\lambda_N(\tau_N-)\Big]\eta_N(\tau_N-),\qquad(13)\end{aligned}$$

where

$$A_i=\frac{\partial H_i}{\partial u_i},\qquad\text{and}\qquad B_i=\frac{\partial\phi_i}{\partial w_i}+\mu_i\frac{\partial F}{\partial w_i}\qquad(14)$$

$$\begin{aligned}C_i=&\Big[L_i(x_i,u_i)-L_{i+1}(x_{i+1},u_{i+1})\Big]_{\tau_i}+\\
&+\Big[\mu_i\frac{\partial F}{\partial x_i}f_i(\tau_i-)-\mu_i f_{i+1}(\tau_i+)+\frac{\partial\phi_i}{\partial x_i}f_i(\tau_i-)\Big].\qquad(15)\end{aligned}$$

Here we used the fact that $\phi_N(x_N(\tau_N-),w_N) = \Phi_N(x_n(\tau_N))$ and $\eta_1(0+) = 0$. The computation of the perturbations $\{\eta_i\}$ is avoided by choosing

$$\mu_i = \lambda_{i+1}(\tau_i+), \qquad (16)$$

$$\lambda_i(\tau_i-) = \mu_i\frac{\partial F_i}{\partial x_i}+\frac{\partial\phi_i}{\partial x_i},\ \text{and} \qquad (17)$$

$$\lambda_N(\tau_N-) = \frac{\partial\Phi}{\partial x_N}. \qquad (18)$$

These conditions specify the boundary conditions of the co-state defined by (12).

With this choice of the co-state, the first order variation of J reduces to

$$\delta J=\sum_{i=1}^{N}\int_{\tau_{i-1}}^{\tau_i}A_i\nu_i dt+\sum_{i=1}^{N-1}B_i\omega_i+\sum_{i=1}^{N-1}C_i\theta_i. \qquad (19)$$

Since θ_i, ω_i, and ν_i are independent, the necessary conditions for optimality are the vanishing of A_i's, B_i's, and C_i's in (13). These results are summarized in a theorem below:

Theorem 3.1: Given a multi-dimensional hybrid system of the form (3) and (4), an extremum to the performance index J in (5) is attained when the control variables u_i, for $i = 1,\ldots,N$, τ_i and w_i, for $i = 1,\ldots,N-1$, are chosen as follows:

Euler-Lagrange Equations: $\dot{\lambda}_i = -\frac{\partial H_i}{\partial x_i}(x_i,\lambda_i,u_i)$, with

$t \in (\tau_{i-1}, \tau_i)$, for $i = 1, \ldots, N$.
Boundary Conditions: $\lambda_N(\tau_N-) = \frac{\partial \Phi}{\partial x_N}$, and $\lambda_i(\tau_i-) = \lambda_{i+1}(\tau_i+)\frac{\partial F_i}{\partial x_i} + \frac{\partial \phi_i}{\partial x_i}$, for $i = 1, \ldots, N-1$.
Optimality Conditions: $\frac{\partial H_i}{\partial u_i} = 0$, $\frac{\partial \phi_i}{\partial w_i} + \lambda_{i+1}(\tau_i+)\frac{\partial F}{\partial w_i} = 0$, and $H_i(\tau_i-) - H_{i+1}(\tau_i+) = 0$, where H_i is the Hamiltonian $H_i(x_i, \lambda_i, u_i) = L_i(x_i, u_i) + \lambda_i f_i(x_i, u_i)$.

C. Numerical Algorithms

Now that we have derived the necessary conditions for optimality, we introduce numerical algorithms that utilize these conditions to attain optimal control values:

- Initialize with a guess of the control variables $\tau_i^{(0)}$, $w_i^{(0)}$, for $i = 1, \ldots, N-1$, and $u_i^{(0)}(t)$ with $t \in [\tau_{i-1}^{(0)}, \tau_i^{(0)})$ for $i = 1, \ldots, N$, and let $p = 0$.
- `while` $p < 1$ `or` $|J^{(p)} - J^{(p-1)}| < \epsilon$
  1. Compute the state trajectories $x_i(t)$, for $i = 1, \ldots, N$, and cost $J^{(p)}$ forward in time from 0 to T using (3), (4), and (5).
  2. Compute the co-states $\lambda_i(t)$, for $i = 1, \ldots, N$, backward in time from T to 0 using (12), and (16) - (18).
  3. Compute A_i, B_i, C_i for $i = 1, \ldots, N$ using (14)-(15).
  4. Update the control variables τ_i and w_i as follow :
$$\tau_i^{(p+1)} = \tau_i^{(p)} - \gamma_\tau^{(p)} C_i,$$
$$w_i^{(p+1)} = w_i^{(p)} - \gamma_w^{(p)} B_i,$$
for $i = 1, \ldots, N-1$,where $\gamma_\tau^{(p)}$ and $\gamma_w^{(p)}$ are step size parameters.
  5. Update the control u_i using the `update-u` sub-function (defined below):
$$u_i^{(p+1)} = \texttt{update-u}(u_i^{(p)}).$$
  6. $p = p + 1$
- `end while`

In the algorithm above, γ denotes the step-size, and an efficient method among others is to use the Armijo step-size [15]. This algorithm is similar to a gradient descent algorithm, however there is one big distinction. The τ_i's and w_i's can be readily updated in the negative gradient direction as usual. However, the continuous control vector u_i cannot be updated using the standard approach because of the change in dimensions between modes. To see why this happens, consider the situation depicted in Figure 4. Here if we update the control u_i using the usual update method, the $u_i^{(p+1)}(t) \in \mathbb{R}^{m_i}$ when $t \in [\tau_{i-1}^{(p)}, \tau_i^{(p)})$. However, upon updating the switching times, there will be two regions of conflict assuming the switching times change.

There are four distinct cases of conflict that can occur for each control u_i. To address the update issue and the regions of conflict, we propose the following `update-u` function:

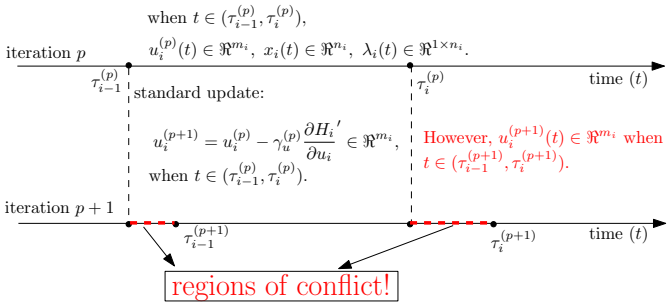

Fig. 4. Depicted here is a situation where the standard update method leads to a conflict in dimensions of the control u_i.

$u_i^{(p+1)} = \texttt{update-u}(u_i^{(p)})$
- $u_{temp}(t) = u_i^{(p)} - \gamma_u^{(p)} \frac{\partial H_i}{\partial u_i^{(p)}}'$
- `if` $\left(\tau_{i-1}^{(p+1)} \geq \tau_{i-1}^{(p)} \;\&\; \tau_i^{(p+1)} \geq \tau_i^{(p)}\right)$
  - $u_i^{(p+1)}(t) = u_{temp}(t)$; $t \in [\tau_{i-1}^{(p+1)}, \tau_i^{(p)})$,
  - $u_i^{(p+1)}(t) = u_{temp}(\tau_i^{(p)}) + (t - \tau_i^{(p)})\dot{u}_{temp}(\tau_i^{(p)})$; $t \in [\tau_i^{(p)}, \tau_i^{(p+1)})$.
- `elseif` $\left(\tau_{i-1}^{(p+1)} \geq \tau_{i-1}^{(p)} \;\&\; \tau_i^{(p+1)} \leq \tau_i^{(p)}\right)$
  - $u_i^{(p+1)}(t) = u_{temp}(t)$; $t \in [\tau_{i-1}^{(p+1)}, \tau_i^{(p+1)})$.
- `elseif` $\left(\tau_{i-1}^{(p+1)} \leq \tau_{i-1}^{(p)} \;\&\; \tau_i^{(p+1)} \geq \tau_i^{(p)}\right)$
  - $u_i^{(p+1)}(t) = u_{temp}(t)$; $t \in [\tau_{i-1}^{(p)}, \tau_i^{(p)})$,
  - $u_i^{(p+1)}(t) = u_{temp}(\tau_i^{(p)}) + (t - \tau_i^{(p)})\dot{u}_{temp}(\tau_i^{(p)})$; $t \in [\tau_i^{(p)}, \tau_i^{(p+1)})$,
  - $u_i^{(p+1)}(t) = u_{temp}(\tau_{i-1}^{(p)}) + (\tau_{i-1}^{(p)} - t)\dot{u}_{temp}(\tau_{i-1}^{(p)})$; $t \in [\tau_{i-1}^{(p+1)}, \tau_{i-1}^{(p)})$.
- `elseif` $\left(\tau_{i-1}^{(p+1)} \leq \tau_{i-1}^{(p)} \;\&\; \tau_i^{(p+1)} \leq \tau_i^{(p)}\right)$
  - $u_i^{(p+1)}(t) = u_{temp}(t)$; $t \in [\tau_{i-1}^{(p)}, \tau_i^{(p+1)})$,
  - $u_i^{(p+1)}(t) = u_{temp}(\tau_{i-1}^{(p)}) + (\tau_{i-1}^{(p)} - t)\dot{u}_{temp}(\tau_{i-1}^{(p)})$; $t \in [\tau_{i-1}^{(p+1)}, \tau_{i-1}^{(p)})$.
- `end if`

The idea here is to *trim* and *extend* the control u_i as necessitated by the change in the switching times. The extension is done by using a first-order Taylor approximation. The instance shown in Figure 4 corresponds to the when $\tau_{i-1}^{(p+1)} > \tau_{i-1}^{(p)}$ and $\tau_i^{(p+1)} > \tau_i^{(p)}$. In this case, since τ_{i-1} increased, the beginning (e.g. when $t = [\tau_{i-1}^{(p-1)}, \tau_{i-1}^{(p)})$) is trimmed. Also since τ_i increased, the end (e.g. when $t = [\tau_i^{(p-1)}, \tau_i^{(p)})$) must be extended. The other cases are similar.

IV. OPTIMAL CONTROL OF ICE SKATER

In this section, we derive the optimal control of the ice skater model presented in Section II using the algorithms from the previous section. In particular, we assume the skater has an initial velocity of $v_c(0) = 1\ m/s$ and it is desired to achieve a velocity of $v_d = 3\ m/s$ in T seconds while minimizing the energy expenditure (or work done). With this goal in mind, the following performance index is proposed:

$$J = \int_0^T C_1(u(t)D(t))dt + C_2(v_c(T) - v_d)^2, \qquad (20)$$

where C_1 and C_2 are scalar weights, $u(t)$ and $D(t)$ represent the force applied by the skater and the distance travelled by the skates, respectively. In order to fit problem into the general framework presented in Sections II and III. First, note that $u(t) = 0$ in the GL and GR modes, hence $L(t) = 0$ in these modes. The instantaneous cost during the SL and SR mode is $L(t) = C_1\big(u(t)\sin(\theta(t))\big(x_l(t) + x_r(t)\big) + u(t)\cos(\theta(t))\big(y_l(t)+y_r(t)\big)\big)$, where $x_l(t), y_l(t), x_r(t), y_r(t)$ are the x and y coordinates of the left and right skates, respectively and $\theta = \tan^{-1}(\frac{x_l - x_r}{y_l - y_r})$. Moreover, we note that $\phi_i(x_i(\tau_i-), w_i) = 0$ and $\Phi(x_N(\tau_N)) = C_2(v_c(\tau_N) - v_d)^2$.

For the purpose of the simulation, it is assumed that the state transitions (F_i) are autonomous (e.g. no discrete control w_i), and also $\alpha_l = \frac{\pi}{6}$ and $\alpha_r = -\frac{\pi}{6}$ are assumed fixed. In this case, the control consists of the switching times τ_i and the continuous control $u_i(t)$. We will start in the SL mode and transition between different modes as specified in Figure 2. In the simulation, the initial skate positions are $x_0 = [0, 0, 1, 0.25, -0.25, 1]$ and we assume an skater of average body type [16]: $M = 40\ kg$, $m = 20\ kg$, $\mu_k = 0.157\ \frac{kg}{m}$, $v_d = 3\ \frac{m}{s}$, $T = 3\ s$, $C_1 = 0.01$, and $C_2 = 50$. Figure 5 shows the optimal switching times by displaying the active mode as a function of time, and Figure 6 depicts the trajectory using the optimal control u_i and optimal switching times τ_i.

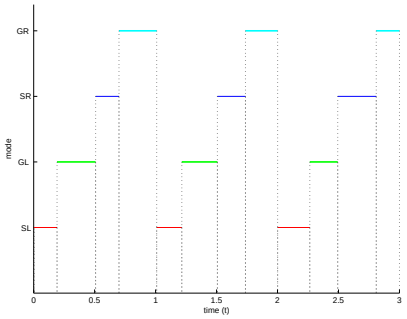

Fig. 5. Depicted is the active mode as a function of time for the optimal switching times.

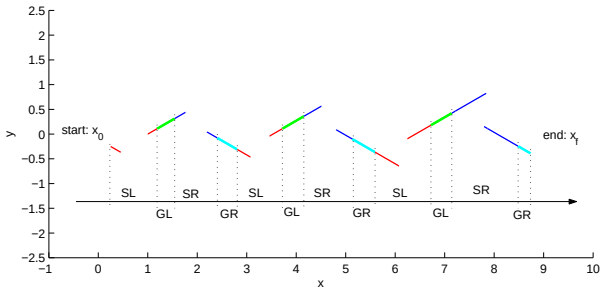

Fig. 6. Depicted is the optimal trajectory staring in SL mode and switching between the GL, SR, GR modes.

V. CONCLUSIONS

In this paper, we presented an algorithmic framework for the optimal control of systems that experience changes in dimensions of the state and input spaces between different modes of operation. These changes in the dimensions can be imposed as infinite-dimensional state constraints, but these constraint typically add significant computational overhead. Instead, we introduced a non-standard Multi-Mode, Multi-Dimension (M^3D) model and derived optimality conditions for such systems using variational arguments. We moreover derived a detailed M^3D model for an ice-skater, and demonstrated the viability of the presented methods through an optimal control example of the ice-skater.

REFERENCES

[1] Junho Choi and J.W. Grizzle, Planar Bipedal Walking with Foot Rotation, In *American Control Conference*, Portland, Oregon, June 2005.

[2] F. Bullo and M. Zefran. On modeling and locomotion of hybrid mechanical systems with impacts. In *IEEE Conf. on Decision and Control*, Tampa, FL, December 1998.

[3] R. Ghosh and C. J. Tomlin, Symbolic reachable set computation of piecewise affine hybrid automata and its application to biological modeling: Delta-Notch protein signaling, In *IEE Transactions on Systems Biology*, Volume 1, Number 1, pp. 170-183, June 2004.

[4] E. Sontag, Molecular Systems Biology and Control: A Qualitative-Quantitative Approach, In *IEEE Conf. on Decision and Control*, Seville, Spain, December 2005.

[5] T.D. Murphey and J.W. Burdick, Feedback Control Methods for Distributed Manipulation Systems that involve Mechanical Contacts

[6] H.J. Sussmann. Set-Valued Differentials and the Hybrid Maximum Principle. *IEEE Conference on Decision and Control*, Vol. 1, pp. 558 -563, Dec. 2000.

[7] M.S. Shaikh and P.E. Caines. On the Optimal Control of Hybrid Systems: Optimization of Trajectories, Switching Times and Location Schedules. In *Proceedings of the 6th International Workshop on Hybrid Systems: Computation and Control*, Prague, The Czech Republic, 2003.

[8] A. Bemporad, F. Borrelli, and M. Morari. On the Optimal Control Law for Linear Discrete Time Hybrid Systems. In *Hybrid Systems: Computation and Control*, M. Greenstreet and C. Tomlin, Editors, Springer-Verlag Lecture Notes in Computer Science, Number 2289, pp. 105-119, 2002.

[9] M. Egerstedt, Y. Wardi, and H. Axelsson. "Transition-Time Optimization for Switched Systems". *IEEE Transactions on Automatic Control*, Vol. 51, No. 1, pp. 110-115, Jan. 2006.

[10] X. Xu and P.J. Antsaklis, "A Dynamic Programming Approach for Optimal Control of Switched Systems". *Proceedings of the 39th IEEE Conference on Decision and Control*, pp. 1822-1827, Sydney, Australia, December, 2000.

[11] B. Lincoln and A. Rantzer. "Optimizing Linear Systems Switching." *IEEE Conference on Decision and Control*, pp. 2063 2068, Orlando, FL, 2001.

[12] D. Hristu-Varsakelis, R. Brockett. " Experimenting with hybrid control", in *Control Systems Magazine*, Vol.22, No. 1, pp. 82-95, Feb. 2002.

[13] E. I. Verriest, "Multi-Mode Multi-Dimensional Systems," *International Symposium on the Mathematical Theory of Networks and Systems*, Kyoto, Japan, July 2006.

[14] J.J de Koning, G de Groot and G. J van Ingen Schenau, "Ice Friction during speed skating", *J. Biomechanics* Vol. 25, No.6, pp.565-571, 1992.

[15] L. Armijo. Minimization of Functions Having Lipschitz Continuous First-Partial Derivatives. *Pacific Journal of Mathematics*, Vol. 16, ppm. 1-3, 1966.

[16] G. J van Ingen Schenau, "The influence of air friction in speed skating", *J. Biomechanics* Vol. 15, No.6, pp.449-458, 1982.